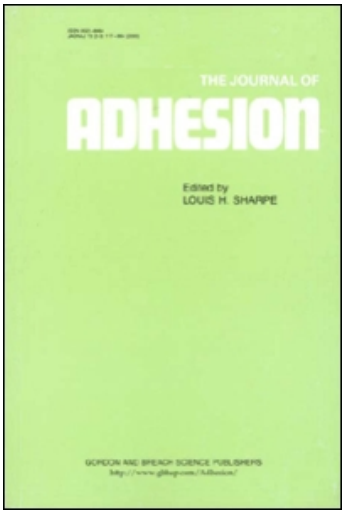

The Journal of Adhesion
Publication details, including instructions for authors and subscription information:
http://www.informaworld.com/smpp/title~content=t713453635

Factors Affecting the Durability of Ti-6Al-4V/Epoxy Bonds

Jennifer A. Filbey[ab]; J. P. Wightman[a]
[a] Department of Chemistry and Center for Adhesion Science, Virginia Polytechnic Institute and State University, Blacksburg, VA, U.S.A. [b] Centre de Recherches sur la Physico-Chimie des Surfaces Solides, CNRS, Kennedy, Mulhouse, France

To cite this Article Filbey, Jennifer A. and Wightman, J. P.(1989) 'Factors Affecting the Durability of Ti-6Al-4V/Epoxy Bonds', The Journal of Adhesion, 28: 1, 1 — 22
To link to this Article: DOI: 10.1080/00218468908030166
URL: http://dx.doi.org/10.1080/00218468908030166

J. Adhesion, 1989, Vol. 28, pp. 1–22
Reprints available directly from the publisher
Photocopying permitted by license only

Printed in the United Kingdom

Factors Affecting the Durability of Ti–6Al–4V/Epoxy Bonds

JENNIFER A. FILBEY† and J. P. WIGHTMAN

Department of Chemistry and Center for Adhesion Science, Virginia Polytechnic Institute and State University, Blacksburg, VA 24061, U.S.A.

(Received April 27, 1988, in final form November 7, 1988)

Factors influencing the durability of Ti–6Al–4V/epoxy interphases were studied by determining chemical and physical properties of Ti–6Al–4V adherend surfaces and by characterizing the strength and durability of Ti–6Al–4V/epoxy bonds.

Ti–6Al–4V adherend surfaces were oxidized either by chemical etch or anodization. Four principal pretreatments were studied: chromic acid anodization (CAA), sodium hydroxide anodization (SHA), phosphate fluoride acid etch (P/F) and TURCO basic etch (TURCO). The oxides were characterized by SEM, STEM, profilometry, contact angles and XPS.

All adhesive bonding was carried out using a structural epoxy, FM-300U. Both lap shear and wedge test samples were tested in hot, wet environments. The results lead to the conclusion that the interfacial area between the adhesive and adherend is the primary factor affecting bond durability.

KEY WORDS Ti–6Al–4V; durability; bonding with epoxy adhesive; adhesion; wedge test; stress durability test.

I. INTRODUCTION

In an adhesive bond, dissimilar materials are brought together to form an interface. Several molecular layers in one material will be influenced by the presence of the other material. Understanding the chemistry and physical structure of this interface region or "interphase" is vital in understanding the interaction between the materials.

The chemistry and topography of a metal adherend surface is primarily determined by the method of preparing the surface prior to bonding. The pretreatment will affect the surface chemical composition, roughness, acidity/basicity, surface energy, oxide thickness, and mechanical properties. The chemical composition of the polymeric adhesive will dictate the mobility of the polymer chains during bonding and thus the ability of functional groups to interact with the metal surface.

† Present address: Centre de Recherches sur la Physico-Chimie des Surfaces Solides, CNRS, 24 avenue du Président Kennedy 68200 Mulhouse, France

The interactions occurring at the interface will ultimately determine the performance of the adhesive bond. In load-bearing adhesive bonds exposed to heat and humidity, good durability is imperative for continued integrity of the structure. One of the primary goals in adhesion science today is to predict real world performance from modeling studies of adhesively-bonded samples. To model effectively, however, the parameters affecting the system must first be established.

The objective of the work described in this paper was to determine the factors which affect the hot-wet durability of Ti-6Al-4V/epoxy bonds. The physical and chemical properties of different Ti–6Al–4V oxide surfaces were studied and the hydrothermal durability of the Ti–6Al–4V/epoxy bonds determined.

II. EXPERIMENTAL

A Materials

Ti–6Al–4V was the metal alloy used in this study. Three forms were used—lap shear coupons supplied by personnel at NASA–Langley Research Center, $2.54 \times 12.7 \times 0.13$ cm; wedge coupons supplied by RMI Titanium, $2.54 \times 15.24 \times 0.38$ cm; and foil purchased from Arnold Subsidiary Magnetics and Electronics, Inc., 0.0038 cm thick. A 175°C cure, rubber-modified, structural epoxy unsupported film adhesive, FM-300U (American Cyanamid) was used for all adhesive bonding. Part of the FM-300 formulation is a brominated diglycidylether of bis-phenol A, which allowed the bromine to be used as a tag in the XPS studies. All chemicals unless otherwise indicated were obtained from Fisher Scientific Company.

B Sample preparation

The Ti–6Al–4V adherends were pretreated by four methods prior to analysis or adhesive bonding—chromic acid anodization (CAA); sodium hydroxide anodization (SHA); phosphate/fluoride acidic etch (P/F); or TURCO[1] basic etch (TURCO). All treatments were preceded by gritblasting the titanium surfaces. Details of the pretreatment procedures are listed in Appendix A. The designation PSHA indicates a pickling step preceded anodization in the SHA treatment.

C Instrumental techniques

The surface topography of pretreated Ti–6Al–4V surfaces was studied using SEM and STEM. Pretreated samples were punched as 0.95 cm diameter disks and sputter coated with 20 nm of gold prior to analysis on a JOEL JSM 35C electron microscope. This coating reduced the effect of charging of the sample by the electron beam.

STEM pictures were taken in the SEM mode on a Philips EM-420T electron microscope. The term STEM is used to denote high-resolution scanning electron

microscopy. Ti–6Al–4V foil was pretreated and cut to 3×8 mm pieces. The samples were conductive, so coating the samples to prevent charging was not necessary.

Chemical composition and reproducibility of surface pretreatments was determined by XPS. After adhesive bonds had been tested, the failure surfaces were also analyzed by XPS to determine the locus of failure. Due to the availability of instruments, spectra were obtained using either a KRATOS XSAM 800 or a PHI 5300 ESCA system, both with a magnesium X-ray anode at a power of 250 W. The pretreated and failure surfaces were 0.95 cm in diameter.

Some failure surfaces were analyzed by Auger electron spectroscopy using a Perkin–Elmer PHI 610 scanning Auger microprobe with an electron beam voltage of 3 to 5 kV and a current of 0.05 μA. Samples were depth propfiled by argon ion sputtering with an ion beam current of 0.2 μA.

D Roughness

The micrometer roughness of pretreated Ti–6Al–4V coupons and foils was determined using a Taylor–Hobson Talysurf 4 Profilometer. A diamond stylus measured the average peak-to-valley distance as well as giving a record of the profile.

E Contamination

Ti–6Al–4V coupons were pretreated, dried and hung in the laboratory environment. The contact angle of water on the surfaces was measured periodically until a contact angle greater than 10 degrees occurred.

F. Surface energy determination

The surface energy of pretreated Ti–6Al–4V samples was determined by contact angle measurements using a two-phase method as described by Carré and Schultz.[2] Ti–6Al–4V coupons, pretreated by one of three pretreatments—CAA, P/F, or TURCO—were placed in a hot plate oven at 110°C for at least 48 h immediately following pretreatment. The oven was then turned off and the coupons allowed to cool to room temperature. The room-temperature coupon was then immersed in hexane, octane, decane or hexadecane in a glass container at room temperature. A 8 μl water drop was placed on the immersed Ti–6Al–4V surface by a syringe needle held approximately 3 mm above the Ti–6Al–4V surface. The contact angle of the water drop on the immersed Ti–6Al–4V sample was measured by a goniometer telescope, through the glass container, 15 seconds after the drop had been applied to the surface.

Corrections for roughness and porosity of the Ti–6Al–4V surfaces used the method reported in Ref. 2. The pretreated surfaces and acid-cleaned glass were coated with 100 nm of gold using an SPI sputter coater. The contact angle of a drop of formamide on each surface was measured. The area covered by pores on

the CAA surface was determined from STEM photomicrographs by counting the number of pores per unit area using an average pore diameter of 40 nm.

Once the dispersive (γ^D) and polar (γ^P) components of the Ti–6Al–4V surfaces were obtained, where $\gamma = \gamma^P + \gamma^D$, the surface energies were used to calculate the thermodynamic work of adhesion between x and y using the Dupré equation:

$$W_A = \gamma_x + \gamma_y - \gamma_{xy} \tag{1}$$

The work of adhesion of an epoxy/Ti–6Al–4V bond in air (W_A) and in water, (W_{AW}), was calculated using the following equations, assuming values of 37.2 and 8.3 mJ/m^2 for γ_E^D and γ_E^P of the epoxy, respectively.[3]

$$W_A = 2((\gamma_{Ti}^D \gamma_E^D)^{1/2} + (\gamma_{Ti}^P \gamma_E^P)^{1/2}) \tag{2}$$

$$W_{AW} = 2(\gamma_W - (\gamma_{Ti}^D \gamma_W^D)^{1/2} - (\gamma_{Ti}^P \gamma_W^P)^{1/2} - (\gamma_E^D \gamma_W^D)^{1/2} - (\gamma_E^P \gamma_W^P)^{1/2} + (\gamma_{Ti}^D \gamma_E^D)^{1/2} + (\gamma_{Ti}^P \gamma_E^P)^{1/2}) \tag{3}$$

G Adhesive bonding

1 *FM-300U characterization* Dynamic mechanical thermal analysis (DMTA) was used to study cured FM-300U films before and after 30-day exposure to 80°C water. A Polylab DMTA analyzer was used at 1 Hz from 0° to 200°C, thus monitoring the molecular relaxation known as the alpha transition, or T_g, of the polymer.

2 *Pore penetration study* To determine if the epoxy penetrated the CAA porous oxide, a piece of Ti–6Al–4V foil was anodized by the CAA pretreatment. FM-300U film was placed on top of the CAA foil, covered with a Teflon sheet and bonded at 175°C for 1.5 h. Because of the foil's flexibility, the epoxy/foil laminate could be peeled apart, creating a metal failure surface (MFS) and an adhesive failure surface (AFS). These surfaces were studied by STEM, XPS, and AES with depth profiling.

3 *Lap shear test* Lap shear coupons (2.54 × 12.7 × 0.13 cm) were pretreated and bonded with FM-300U epoxy. The pretreated surfaces were not primed with an organic primer. The lap shear coupons were placed in a jig set for 1.27 × 2.54 cm overlap with a bondline thickness of 0.076 cm. The FM-300U film was cut as 1.9 × 2.54 cm pieces to provide adhesive fillets, thus reducing stress concentration at the ends of the coupons. The jig was placed in a Pasadena Hydraulics platen press and heated from room temperature to 175°C under 13.8 MPa bonding pressure for 1.5 h. The heat was turned off and the joints allowed to cool to room temperature under pressure. All lap shear joints were aged in laboratory atmosphere for at least 10 days before testing. Lap shear bonds were pulled to break at room temperature on an Instron at a crosshead speed of 0.127 cm per min. The failure surfaces were studied by XPS and SEM to determine the locus of failure.

4 *Stress durability test* Lap shear joints, as described above, were also loaded to 40% of the average breaking strength by a spring of known force constant. The loaded joints were placed in a 3M stress-durability cabinet at 80°C, 95% r.h. and the time for the joint to fail was measured. The failure surfaces were studied by XPS to determine the locus of failure.

5 *Wedge test* Wedge coupons, $2.54 \times 15.24 \times 0.38$ cm, were pretreated and bonded with two layers of FM-300U cut to the same dimensions as the wedge coupons, leaving 0.5 cm clear at each end. The thickness of the bond line was controlled using Teflon film spacers yielding a bond line thickness of 0.038 cm. The wedge joints were placed in a platen press and heated from room temperature to 175°C under 1.72 MPa bonding pressure for 1.5 h. The heat was turned off and the joints allowed to cool to room temperature under pressure. A Ti-6Al-4V wedge was driven into one end of the wedge joint with a hammer causing an initial crack to propagate. The position of the initial crack was measured with a ruler to the nearest 0.5 mm and the joint placed in an environment. The crack propagation with time was then monitored periodically by removing the joint from the environment to measure the crack.

Marceau and coworkers proposed this variation of the uniform double cantilever beam test—the wedge test.[4] Instead of a constant load being applied to the double cantilever beam sample, a constant displacement, namely the wedge, is applied to the wedge sample. The strain energy release rate, G_1, takes on a different meaning in the wedge test. For the constant load, double cantilever beam test, G_1 is the energy required for crack propagation; whereas, for the constant displacement wedge test G_1 is the energy for crack arrest. As the crack length increases, the strain energy release rate or G_1 decreases, thus yielding a potential for defining "threshold values" for G_1.[4] G_1 is calculated for the wedge test as shown below:[4,5]

$$G_1 = \frac{y^2 M h^3 (3(a + 0.6h)^2 + h^2)}{16((a + 0.6h)^3 + ah^2)^2} \tag{4}$$

where y is the displacement at load point or the wedge thickness, 0.38 cm; a is the distance from load point to crack tip, h is the height or thickness of the adherend beam, 0.38 cm; and M is the modulus of the adherend beam, 1.14×10^{11} Pa. The environments included 80°C, 95% r.h. and 95°C, water immersion.

III RESULTS AND DISCUSSION

A Chemical composition of Ti-6Al-4V oxides

In any study of the durability of adhesive bonds using pretreated adherends and one adhesive, good chemical reproducibility of surface preparation is imperative to assure that variations in performance are not, in fact, due to variations in the chemical composition of the adherend surface. The chemical composition of the pretreated oxides was therefore studied by XPS.

TABLE I
Chemical reproducibility of CAA, P/F and TURCO pretreated Ti–6Al–4V adherends

Pretreatment	Element	B.E. (ev)	±95%	Conc.	±95%
CAA	C	285.0	—	49	7.3
	O	530.4	0.1	37	4.3
	Ti	458.8	0.1	11	2.4
	F	685.0	0.2	2.7	0.9
P/F	C	285.0	—	46	10.8
	O	530.4	0.3	41	8.3
	Ti	458.6	0.2	10	2.6
	P	133.1	0.3	2.1	0.6
TURCO	C	285.0	—	52	9.2
	O	530.0	0.5	36	8.0
	Ti	458.5	0.3	5.6	1.9
	Si	104.2	0.7	6.2	6.4
	Fe	712.2	2.7	1.1	0.9
SHA	C	285.0	—	31	0.7
	O	530.0	0.1	47	1.4
	Ti	458.5	0.3	9.6	2.1
	Si	102.9	0.1	7.2	1.9
	Ca	347.2	0.1	3.7	1.2
PSHA	C	285.0	—	38	0.7
	O	530.4	0.0	46	0.7
	Ti	458.8	0.1	11	0
	Ca	347.4	0	4.0	2.0

The chemical reproducibility of the pretreatments was investigated for the CAA, P/F, and TURCO pretreatments by statistically analyzing the concentrations and binding energies from eight analyses. Table I lists for each pretreatment, the elements detected, the average binding energy (B.E.) and the average concentration (Conc.), both with a 95% confidence limit. Results from the SHA and PSHA surfaces are also included; however, less than eight analyses were run. No significant differences were observed in the results from the two XPS instruments. The binding energies had confidence limits with narrow ranges. Since the binding energy indicates the chemical bonding state of an element, a small confidence limit shows that the pretreated surfaces were chemically reproducible. The confidence limits for the average concentrations were wider, presumably due to variability of the surface contamination layers, routinely present on high energy surfaces exposed to the laboratory atmosphere.

The elements detected on all pretreated surfaces by XPS were carbon, oxygen and titanium. CAA surfaces contained a small percentage of fluorine, present as an inorganic fluoride from HF used in the anodizing bath; however, chromium, also contained in the anodizing bath, was not detected. The P/F surfaces contained a small percentage of phosphorus from the etch solution but fluorine

was not usually detected. TURCO surfaces contained both silicon and iron; however, XPS did not detect silicon or iron in the TURCO 5578 mixture. An AES mapping of iron showed that iron existed as micron-sized particles on the surface[6]. Ditchek *et al.*[7] also detected iron particles on the TURCO-pretreated surface. When the surface was pickled after gritblasting but before the TURCO treatment, no silicon or iron was detected by XPS. Iron and silicon, therefore, resulted from the gritblast step, and the pickling step removed this iron and silicon contamination. The SHA pretreatment for Ti–6Al–4V is reported by Kennedy *et al.*[8] Their optimum pretreatment conditions were chosen for this study. Silicon and calcium were detected on the SHA surface; however, no sodium from the anodization bath was detected. The silicon was from the gritblasting step; calcium resulted from the tap water rinse used to duplicate the procedure of Kennedy *et al.*[8] so that direct comparison of the SEM photomicrographs could be made.[9] The PSHA surface contained less silicon due to the pickling step.

B Surface topography

The surface topography on a nanometer scale of the CAA, SHA, P/F, and TURCO oxides was studied by STEM. Macroporosity was observed in the anodized surfaces but not with the etched surfaces. Figures 1 to 3 show the STEM photomicrographs of CAA, SHA, and PSHA oxides. The porosity in the PSHA surface appeared to be similar to the CAA surface with pore diameters of approximately 40 nm, while the pores in the SHA surface were not as well defined.

The mechanism of pore formation is believed to involve preferential dissolution which is followed by localized heating of the thin interface.

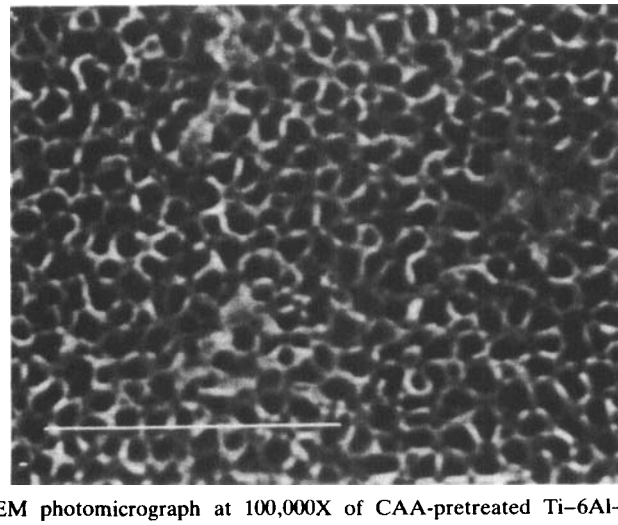

FIGURE 1 STEM photomicrograph at 100,000X of CAA-pretreated Ti–6Al–4V surface. Line represents 500 nm.

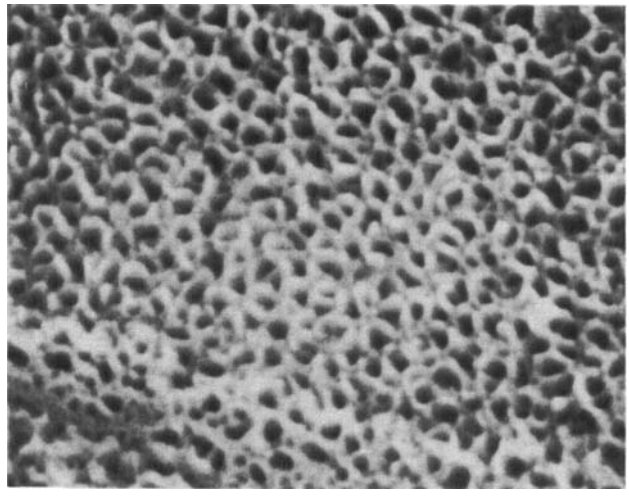

FIGURE 2 STEM photomicrograph at 100,000X of PSHA-pretreated Ti–6Al–4V surface. Same scale as Fig. 1.

In the CAA pretreatment, HF serves as the activator for dissolution.[10] Both CAA and PSHA surfaces are pickled prior to anodization. XPS analysis of pickled Ti–6Al–4V indicates a high concentration of fluorine on the surface, thus allowing for the initiation of well-defined pores. Complementing the presence or absence of fluorine is the difference in current densities between the CAA and SHA procedures. In the CAA process, the current density was controlled; whereas, it was not controlled in the SHA or PSHA treatments. Because the pickling step removed most of the barrier oxide layer, the PSHA surface initially

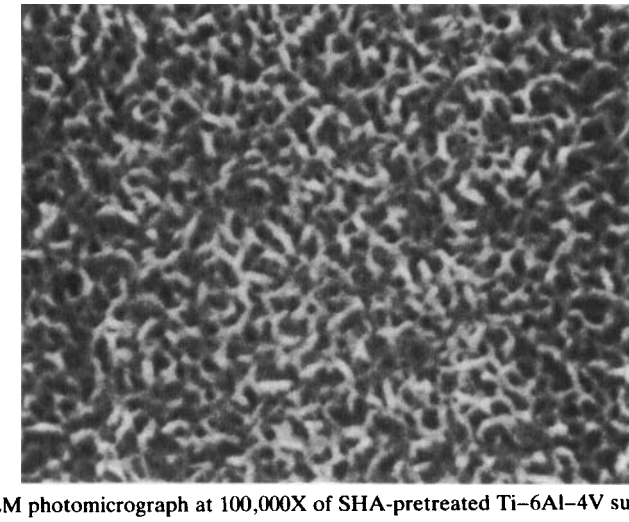

FIGURE 3 STEM photomicrograph at 100,000X of SHA-pretreated Ti–6Al–4V surface. Same scale as Fig. 1.

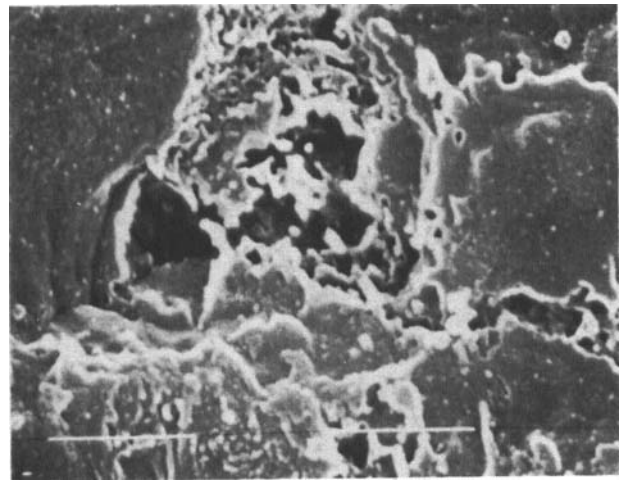

FIGURE 4 STEM photomicrograph at 50,000X of P/F-pretreated Ti-6Al-4V surface. Line represents 500 nm.

showed less resistance to the current. Thus, the effect of localized heating may be more pronounced in the pickled samples than the non-pickled SHA specimens.

Figures 4 and 5 show STEM photomicrographs of the P/F and TURCO surfaces. No porosity, as in the anodized surfaces, was observed on either of these etched surfaces. Porosity was also reported by Ditchek *et al.*[7] for the CAA pretreated Ti-6Al-4V surfaces but not for the P/F or TURCO pretreated Ti-6Al-4V surfaces.

When the non-porous surfaces were observed with scanning electron micro-

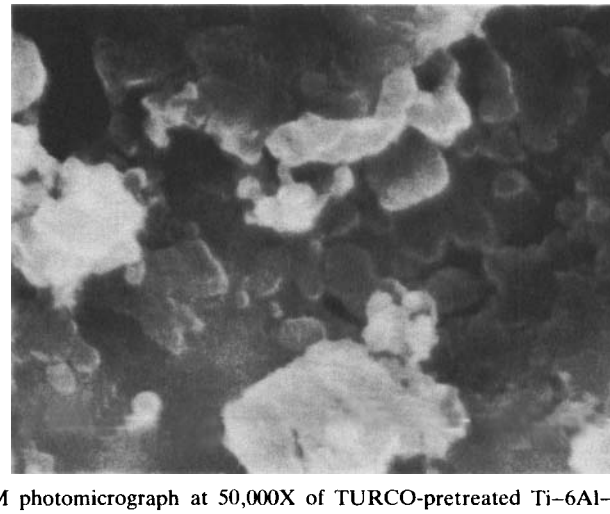

FIGURE 5 STEM photomicrograph at 50,000X of TURCO-pretreated Ti-6Al-4V surface. Line represents 500 nm.

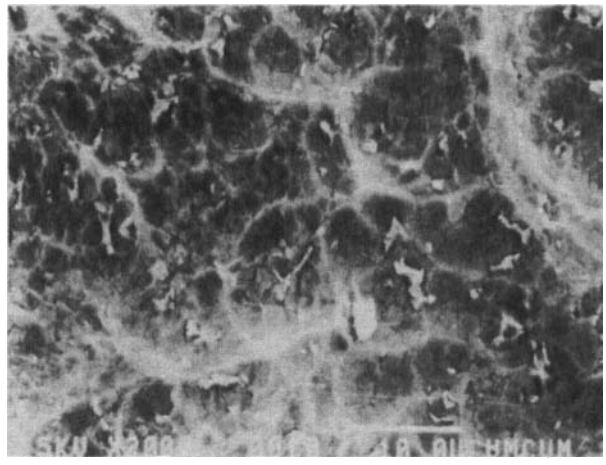

FIGURE 6 SEM photomicrograph at 2000X of P/F-pretreated Ti–6Al–4V. Line represents 10 μm.

scopy at lower magnification relative roughness of the pretreated surfaces could be evaluated. Figures 6 and 7 show the P/F and TURCO pretreated surfaces at 2000 X. Clearly, the TURCO surface was markedly rougher than the P/F surface. The roughness of the anodized surfaces as seen at lower magnifications also differed greatly with the SHA surface markedly rougher than the PSHA or CAA surfaces.[9]

Ditchek *et al.*,[11] using SEM photomicrographs as a basis, rated the roughness of pretreated Ti–6Al–4V with P/F as a smooth surface and TURCO as macrorough on the micrometer level, qualitatively agreeing with the SEM results obtained here for the coupon surfaces.

Another measure of roughness can be obtained using profilometry. While the

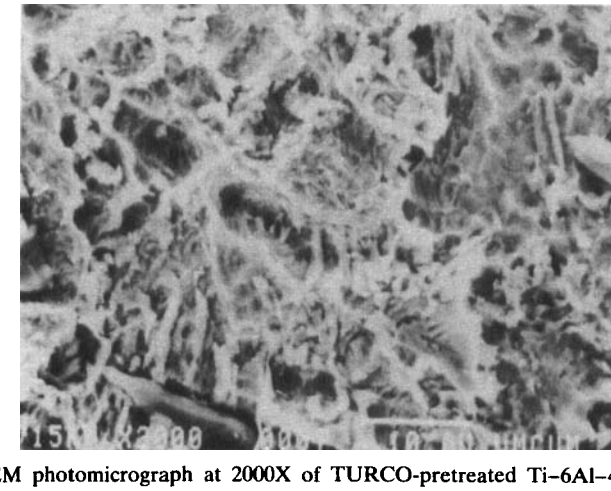

FIGURE 7 SEM photomicrograph at 2000X of TURCO-pretreated Ti–6Al–4V. Line represents 10 μm.

TABLE II
Roughness measurement by profilometry of Ti-6Al-4V lap shear coupon surfaces

Pretreatment	Average peak to valley (μm)	Standard deviation
CAA	2.13	0.26
P/F	2.84	0.28
TURCO	3.36	0.034

profilometer stylus cannot detect roughness on the scale of the porosity observed on the anodized surfaces with STEM, it does provide a relative measure of the roughness on a micrometer scale. Table II lists the average peak-to-valley height with the standard deviation for pretreated coupon surfaces, showing that TURCO is the roughest surface.

The surface topography also may have affected the time for atmospheric contamination which readily occurs on high energy surfaces. Contamination was evaluated by the time for a water contact angle of 10 degrees to be observed on the Ti-6Al-4V surface. A zero contact angle on a freshly-cleaned surface was observed. These times were characteristic for each pretreatment: 12 h for P/F, 31 h for TURCO, and 72 h for CAA. The P/F surface was smoother than the TURCO surface as measured by SEM and profilometry. The CAA surface was also smoother than the TURCO surface; however, porosity is present in the CAA surface. The time for contamination to occur could, therefore, be directly related to the surface area of the Ti-6Al-4V oxide surface, with the order of surface area being P/F < TURCO < CAA, although other factors such as the electronic charge at the surface could also affect contamination rate.

C Pore penetration study

The porous structure in the Ti-6Al-4V surface produced by anodization creates an excellent opportunity for increased surface area for adhesive/oxide interaction. The degree of penetration of epoxy into the porous oxide must be determined for interfacial area arguments to be valid.

The penetration of a fluid into a porous structure can be calculated for a given porous structure and fluid. The epoxy will penetrate a cylindrical pore until the back pressure of trapped air in the pore equals the capillary driving force of filling the pore. The distance of penetration (x) will depend upon the length of the pore (L), the radius of the pore (r), the surface energy of the epoxy (γ_{LV}), the contact angle of the adhesive in the pore (θ) and the atmospheric pressure (P_A) as shown below:[12]

$$x = L\left[1 - \frac{P_A r}{2\gamma_{LV}\cos\theta + P_A r}\right] \tag{5}$$

For a titanium oxide with a pore length of 100 nm and a radius of 20 nm, assuming atmospheric pressure, a surface energy of the epoxy of 45 mJ/m^2 and a

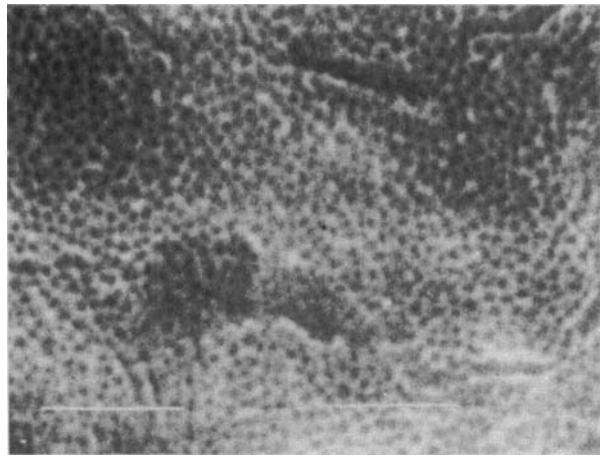

FIGURE 8 STEM photomicrograph at 50,000X of MFS of CAA-pretreated Ti–6Al–4V foil peeled from FM-300U. Line represents 500 nm.

zero contact angle, the epoxy will fill the pore to 98 nm or 98% of the pore will be filled. Thus, theoretically, the epoxy has been shown to penetrate the porous structure of the CAA and SHA surfaces.

A limited number of pore penetration studies have been reported. Packham[12] reports molten polyethylene penetrates 98% of the 10 nm radius pores in an aluminum surface. In cross-section TEM photomicrographs, Brockmann *et al.*[13] have shown that primer penetrates phosphoric acid anodized aluminum pores.

To determine experimentally if the epoxy had penetrated the porous structure, FM-300U was cured on CAA-pretreated Ti–6Al–4V foil and peeled apart. Both the metal failure surface (MFS) and the adhesive failure surface (AFS) were examined by STEM. Figures 8 and 9 show the photomicrographs at 50,000X of

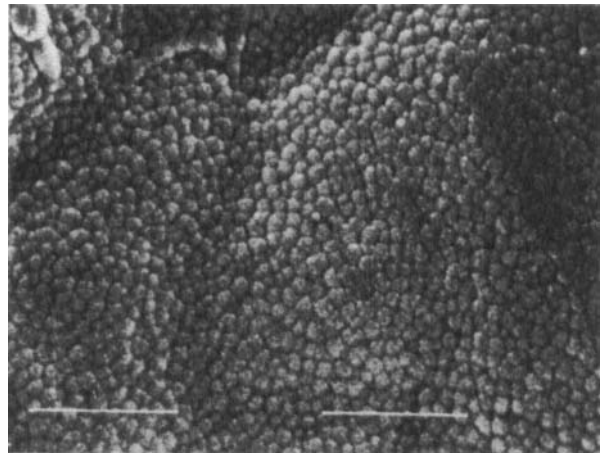

FIGURE 9 STEM photomicrograph at 50,000X of AFS of FM-300U peeled from CAA-pretreated Ti–6Al–4V foil. Line represents 500 nm.

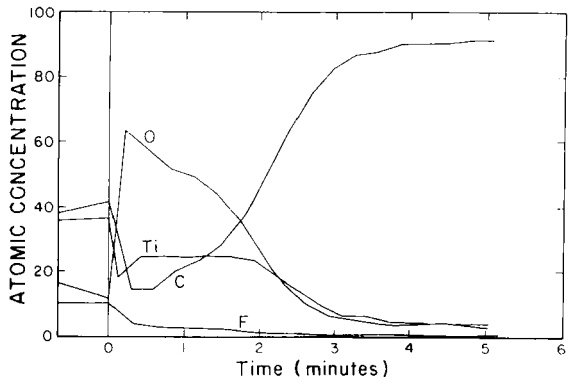

FIGURE 10 AES depth profile of AFS of FM-300U peeled from CAA-pretreated Ti–6Al–4V foil.

the two failure surfaces. The MFS showed a faint evidence of porosity, however, it was unclear as to whether the surface was covered by a thin layer of adhesive or if the majority of the porous structure had been removed. The AFS appeared as if the epoxy had been pulled out of the porous structure. The surface chemical composition was then studied by XPS. Only titanium oxide was present on both surfaces with a high percentage of fluorine. No bromine was detected and the oxygen was indicative of Ti–O bonds. Natan and Venables[14] showed, by AES depth profiling, an increase in fluorine concentration at the oxide/metal interface. The high fluorine concentration indicated that failure had occurred at the base of the porous structure; however, the extent of penetration of the epoxy into the pores was still unclear. The adhesive failure side was then depth profiled with AES. Figure 10 shows the atomic concentration with sputter time. The presence of the carbon signal simultaneously with the titanium and oxygen signals indicated that the epoxy did indeed penetrate the porous structure. This pore penetration is a significant finding because it shows that the interfacial area between the adhesive and oxide is greatly enhanced by the presence of pores.

D Lap Shear Test

1 *Lap shear strength* Strength-to-break measurements were done on lap shear joints made from CAA, P/F, and TURCO pretreated Ti–6Al–4V. The average breaking strengths with the 95% confidence limits for CAA, P/F, and TURCO were 26 ± 4.5, 25 ± 5.6, and 28 ± 6.2 MPa, respectively. The CAA showed the smallest variability in lap shear strength but the breaking strengths of CAA, P/F and TURCO were not significantly different.

The similarity in bond strength of the CAA, P/F and TURCO bonds could imply that the bond performance of the three pretreated surfaces is similar. The similarity could also imply that the lap shear test is not able to differentiate between pretreated surfaces. As will be discussed in the following section, the durability of bonds made with the three pretreatments varies dramatically. The

lap shear test should not be used to evaluate surfaces for bonding, but rather simply to evaluate adhesive performance.

2 *Locus of failure* Although the lap shear strengths did not differ, the locus of failure changed depending on the pretreatment. For all pretreatments, the failure surfaces appeared to result in a metal failure side (MFS) and an adhesive failure side (AFS). The failure surfaces were subsequently studied by XPS. For the CAA-pretreated coupons, both the MFS and the AFS showed titanium oxide. A titanium metal peak, as well as an oxide peak, was also seen on the MFS showing that the remaining oxide layer was thinner than approximately 5 nm. The oxygen peak occurred at 530.6 eV, indicative of a titanium oxide. The AFS contained a high percentage of fluorine and no bromine was detected. The SEM photomicrographs of the AFS clearly appeared to match the MFS photomicrographs and no epoxy was visible on either side.[6] Thus, because titanium metal was detected, the locus of failure was within the oxide layer, close to the base of the pores, a similar failure to the pore penetration experiment. Figure 11 shows schematically the locus of failure for the CAA samples. These results are in contrast to previously reported results, where the locus of failure was in the adhesive.[5,7] The obvious difference between this study and the others using Ti–6Al–4V and FM-300 is that, in this case, no organic primer was used. Although not conclusive, perhaps the lack of primer was the reason for the oxide failure as the primer could have served to reinforce the fragile porous structure.

The P/F- and TURCO-pretreated bonds showed a locus of failure different from the CAA bonds. Although the failure also appeared to be interfacial, no titanium was detected on either the AFS or the MFS. The oxygen peak at approximately 533 eV indicated carbon-oxygen bonds in the epoxy. Bromine, present in the epoxy, was detected on both the AFS and the MFS and nitrogen

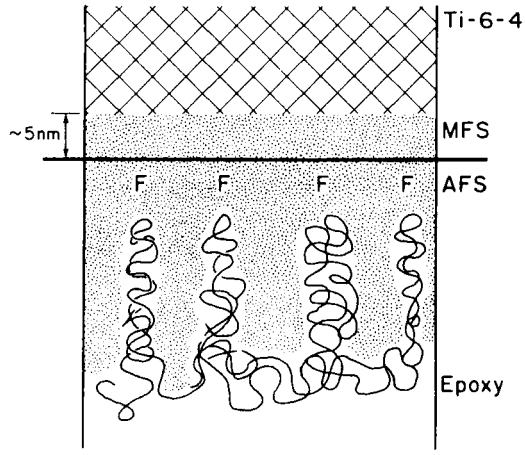

FIGURE 11 Schematic representation of locus of failure for CAA-pretreated Ti–6Al–4V lap shear samples bonded with FM-300U.

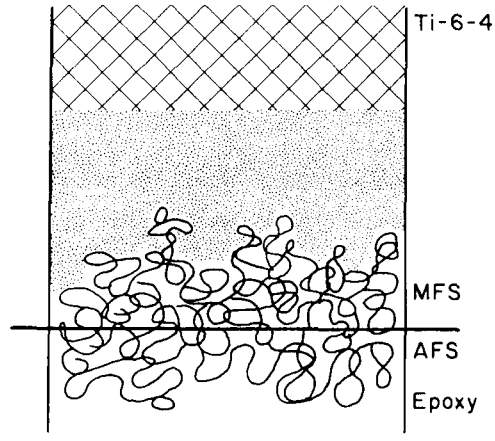

FIGURE 12 Schematic representation of locus of failure for P/F- and TURCO-pretreated Ti-6Al-4V lap shear samples bonded with FM-300U.

was detected in some cases. Epoxy was observed on both MFS and AFS of the TURCO and P/F failure surfaces in the SEM photomicrographs.[6] Thus, the P/F- and TURCO-pretreated samples failed within the adhesive, but visibly close to the metal oxide, as shown schematically in Figure 12. CAA-pretreated surfaces were soaked in boiling water to destroy the porous structure prior to bonding. The failure surfaces were again analyzed by XPS. Failure occurred not within the oxide as in CAA, but in the adhesive similar to the etched P/F and TURCO surfaces, indicating porosity must be present to cause oxide failure.

In summary, the lap shear strengths of bonds made with CAA-pretreated Ti-6Al-4V were similar to those made from TURCO- and P/F-pretreated Ti-6Al-4V, and the locus of failure visually appeared to be similar. However, results from XPS and SEM analyses showed that the locus of failure differed between the anodized and etched surfaces with failure in the oxide for CAA-treated specimens in contrast to cohesive failure in the adhesive in the specimens made using etched surfaces.

E FM-300U characterization

Because the FM-300U epoxy is exposed to hydrothermal conditions in the bond line, it was of interest to determine the effects of an 80°C water soak on the epoxy. The alpha transition of an epoxy film, before and after one month exposure to water at 80°C was studied by DMTA. No significant difference in the mechanical properties of the epoxy film was exhibited before and after water exposure. The wedge and stress durability test results, therefore, were not due to changes in the adhesive mechanical properties.

F Stress durability test

1 *Time to failure* Although the lap shear test was unable to differentiate between good and poor surface pretreatments, the stress-durability test allowed the hydrolytic stability of the lap shear bonds to be tested while under a load of 40% of ambient temperature breaking strength. A notable difference was seen for the three pretreatments in the stress-durability test as shown by the time-to-failure windows in Figure 13. The P/F surface showed poor durability with all bonds breaking in less than one day, while the TURCO and CAA surfaces showed better durability with the CAA being the most durable. Stress-durability results of CAA, TURCO and P/F pretreated Ti–6Al–4V bonds exposed to 60°C, from Wegman and Levi,[15] agree qualitatively with the present results.

Thus the stress-durability test, using lap shear bonds which possessed similar ultimate breaking strengths at ambient conditions as reported in the previous section, showed large differences in durability when exposed to hot, wet conditions.

2 *Locus of failure* The locus of failure for the P/F and TURCO stress-durability samples was determined using XPS. The MFS for both samples showed the presence of titanium oxide. No bromine was detected on these surfaces. The AFS showed the presence of bromine with the O 1s peak indicative of the epoxy. Thus, failure occurred at the interface between the epoxy and the pretreated titanium surface. These results contrast the locus of failure results obtained for the unexposed lap shear samples, where failure occurred within the epoxy.

The CAA stress-durability failure surfaces showed a different failure mode on the edges than in the center of the bond line. XPS analysis indicated interfacial failure around the edges of the failure surface and oxide failure in the center of the failed surface. These results were not unexpected since once approximately

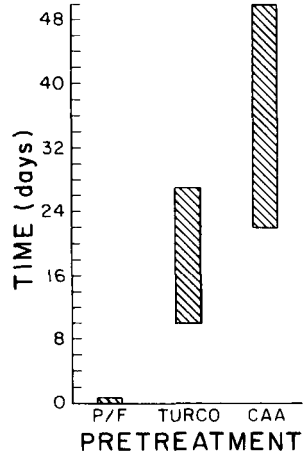

FIGURE 13 Time to failure windows from the stress-durability test at 80°C, 95% r.h.

60% of the bond integrity had been destroyed by moisture around the edges, the remaining center bonded portion could no longer withstand the applied load and rapid deformation occurred similar to the lap shear test, which resulted in a similar failure in the center of the bond.

The presence of moisture weakens the titanium oxide/epoxy interface causing it to be the "weakest link" in the system.

G Wedge test

1 *Crack extension tests* The wedge test also showed sensitivity to surface pretreatment. Ditchek *et al.*[11] reported the durability of CAA, P/F, and TURCO pretreated Ti–6Al–4V which had been primed with an organic primer and exposed to 60°C, 95% r.h. The CAA was found to be the most durable and the P/F the least durable with TURCO showing intermediate durability. It was of interest, therefore, to look at the performance of the same pretreatments under more severe environments, with no primer, which has not been previously reported.

CAA, SHA, TURCO, and P/F samples were exposed in a 80°C, 95% r.h. environment. The CAA, SHA and TURCO samples showed no crack propagation for 14-, 26- and 14-day test periods, respectively. Zero crack growth is also in contrast with previously reported results.[8,16] Once again, no organic primer was used in the present case. In addition, the crack tip was not magnified for observation and thus propagation of less than 0.5 mm was unable to be observed. Cracks did propagate, however, in the P/F samples which showed rapid crack propagation to failure in less than 24 h.

To accelerate the wedge test further, CAA, SHA, TURCO, and P/F surfaces were immersed in 95°C water. After 16 days, the TURCO samples showed the initiation of crack growth, with the crack propagating 0.1 cm, but the CAA and SHA samples showed no propagation. However, for longer exposure times, cracks began to propagate in both the CAA and SHA samples. Thus, results from the stress durability test qualitatively agreed with results from the wedge test with the anodized surfaces being the most durable, followed by TURCO, and finally with the P/F showing poor durability similar to that in 80°C, 95% r.h.

The rate of crack growth *versus* time for P/F samples immersed in 95°C water is shown in Figure 14. There was an initial decrease in the rate of crack growth due to the joint geometry. Because the wedge test is a constant displacement test, as the crack length increases, the load at the crack tip decreases, thus a decreasing rate was expected. After approximately 1.5 h, however, the rate began to increase and continued to increase until failure, thus indicating that the environment was changing the bond integrity.

2 *Strain energy release rate,* G_1 As discussed above, the strain energy release rate (G_1) for the wedge test is the energy for crack arrest and it can, therefore, give an indication of how much energy the bond can absorb without crack propagation. Initial crack lengths were averaged and the 95% confidence limit

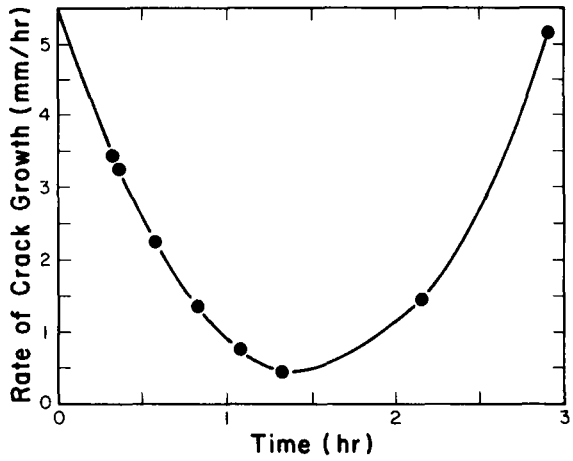

FIGURE 14 Rate of crack extension *versus* time for P/F samples in 95°C water.

found to be 6.0 ± 0.4 cm for CAA, 6.3 ± 0.3 cm for P/F and TURCO. Calculating the corresponding G_1 values with 95% confidence limits yielded 1200 ± 340, 940 ± 180 and 960 ± 160 Pa · m for CAA, P/F, and TURCO, respectively. While the CAA-pretreated samples have a higher average G_1, there was no statistical difference between the initial energy each bond can withstand for the various pretreated samples.

The difference between the pretreatments occurred when the bonds were exposed to the environment. A similar trend in similar dry strengths was observed for the lap shear test. No statistical difference in lap shear strength exists; however, upon exposure to humidity under load, there was a drastic change in durability between pretreatments.

In the 80°C, 95% r.h. environment, the CAA- and TURCO-pretreated samples showed no crack propagation. Therefore, the energy for crack arrest was greater than or equal to approximately 1000 Pa · m. On the other hand, for the P/F samples, the crack never arrested for the entire bond length of 12 cm tested. Thus, the P/F-treated samples could not even withstand 76 Pa · m—the energy at the end of the bond.

3 *Locus of failure* The locus of failure for the P/F-pretreated wedge samples was determined using XPS. The MFS showed no epoxy; titanium, oxygen and carbon were detected with the oxygen binding energy indicative of titanium oxide. The AFS showed only carbon, oxygen, nitrogen and bromine, with binding energies corresponding to that of the neat epoxy. The bonds failed at the epoxy/metal oxide interface, the same locus of failure occurring in the stress durability tests.

With either test—the stress-durability test using the lap shear geometry or the wedge test—the locus of failure for environmentally-exposed bonds was the same—interfacial. These results are a significant finding showing that failure is a function of the interfacial degradation and is independent of the joint geometry.

H Surface energy

A common question asked in durability studies is what is the driving force for water to degrade the interface. The thermodynamic driving force can be determined by measuring the surface energy of the interfacial components.

The polar and dispersive components of the surface free energy were determined for CAA-, P/F-, and TURCO-pretreated Ti–6Al–4V surfaces from interfacial contact angle measurements. Table III lists the values of the dispersive and polar components of the surface energy. The numbers in parentheses are the values obtained when no correction for roughness or porosity is made. Particularly for the porous surface of CAA, there is a significant difference in the γ^P and γ^D values when no correction is made for porosity and roughness. Carré and Schultz[2] found for sulfuric acid anodized (SAA) 5052 aluminum, dispersive and polar components of the surface energy were 125 and 44 mJ/m^2, respectively. For a sealed anodized surface, where the pores have been filled, the dispersive and polar components of the surface energy were 41 and 15 mJ/m^2, respectively. The values obtained for the anodized titanium, while lower, agree qualitatively with the trends of Carré and Schultz. Likewise, the slightly lower values for the etched titanium surfaces compare favorably with their sealed anodized surfaces[2].

TABLE III
Dispersive and polar components of the surface energy of pretreated Ti–6Al–4V, using the geometric mean. γ in mJ/m^2

Pretreatment	γ_s^D	γ_s^P
CAA	87 (4.0)	30 (1.9)
P/F	64 (40)	14 (14)
TURCO	52 (31)	16 (17)

From the polar and dispersive components of the surface energy, the work of adhesion for the epoxy/Ti–6Al–4V and for the water/Ti–6Al–4V interfaces in air was calculated and the values are listed in Table IV. The work of adhesion in air for the CAA-pretreated Ti–6Al–4V/epoxy (146 mJ/m^2) compares well with that of 176 mJ/m^2 for SAA-treated aluminum and the average value (115 mJ/m^2) for

TABLE IV
Work of adhesion in air, W_A, of epoxy/Ti–6Al–4V and water/Ti–6Al–4V interfaces and work of adhesion in water, W_{AW}, of epoxy/Ti–6Al–4V interfaces. W in mJ/m^2

Pretreatment	W_A Epoxy/Ti	W_A Water/Ti	W_{AW} Epoxy/Ti
CAA	146	165	26.6
P/F	119	128	37.7
TURCO	112	124	32.8

the TURCO and P/F pretreatments compares well with 101 mJ/m^2 for sealed SAA-treated aluminum.[2] The calculated work of adhesion for the Ti–6Al–4V/water interface was higher than for the Ti–6Al–4V/epoxy interface. A similar trend was observed in the aluminum system. Thus, titanium has a higher affinity for water than for the epoxy. This affinity can be illustrated by calculation of the work of adhesion of a Ti–6Al–4V/epoxy interface in a water environment.

Table V also lists the work of adhesion for the Ti–6Al–4V/epoxy bond in water (W_{AW}). The calculated work of adhesion was seriously reduced for bonds in a water environment. Thus, thermodynamics predicts a weaker bond between the titanium and epoxy in water than in air, as was demonstrated experimentally in the durability tests.

IV SUMMARY

Factors influencing the durability of Ti–6Al–4V/epoxy interphases were studied by determining chemical and physical properties of Ti–6Al–4V adherend surfaces and by characterizing the strength and durability of Ti–6Al–4V/epoxy bonds.

Good reproducibility of oxide chemical composition was shown as evidenced by XPS analysis. The two anodically-produced oxides were porous, with pore diameters of 40 to 50 nm, while P/F- and TURCO-pretreated adherends showed no porosity. Because the CAA- and SHA-pretreated Ti–6Al–4V adherends were porous, they possessed the highest surface area. For the non-porous oxide surfaces, TURCO was the roughest surface as evidenced by profilometry and SEM and therefore had a higher surface area than the smoother P/F surface. The SHA and CAA pretreatments were equally durable in 80°C, 95% r.h., while the TURCO pretreatment was slightly less durable. The P/F pretreatment exhibited minimal durability in the hot-wet environments.

Some key issues in adhesive bond testing and failure analysis have been addressed. Firstly, the lap shear test was unable to differentiate between different surface pretreatments of Ti–6Al–4V; however, the locus of failure differed between the etched and anodized surfaces. The ability to detect differences in locus of failure in the lap shear test indicated that the failure surfaces were not destroyed in the test itself. Secondly, when hot, wet conditions were introduced to a stressed sample, either in the stress-durability or the wedge tests, significant differences in the durability of pretreatments were observed, with the locus of failure occurring at the epoxy/Ti–6Al–4V oxide interface in all cases. These results lead to a third extremely important issue. For each set of tests reported here, the adhesive, adherend, and environmental conditions remained constant, with the only difference being the surface preparation of the adherend. Predictive modeling of durability, using only bulk properties of adherend and adhesive is, therefore, not sufficient. Interfacial properties must be included to provide an adequate predictive model.

Acknowledgements

The authors would like to acknowledge the following people: Frank Cromer for training in the operation of the PHI XPS and AES and for help in data collection, Steve McCartney for operating the KRATOS XPS and the STEM, and Dr. W. Grant for making available the stress-durability tester.

The authors would also like to acknowledge the Office of Naval Research and NASA-Langley Research Center for financial support of the work. The gifts of Ti-6Al-4V from RMI Titanium, wedge coupons from Martin Marietta Laboratories, and FM-300U from American Cyanamid were appreciated. Enabling funds for the purchase of the surface analysis equipment were provided by the National Science Foundation and Virginia Polytechnic Institute and State University.

References

1. One of the primary components in TURCO 5578 is sodium hydroxide.
2. A. Carré and J. Schultz, *J. Adhesion* **15,** 151 (1983).
3. J. Comyn in *Durability of Structural Adhesives,* A. J. Kinloch, Ed. (Applied Science Publishers, London, 1983).
4. J. A. Marceau, Y. Moji, and J. C. McMilliam, *Adhes. Age* **20**(10), 28 (1977).
5. S. R. Brown and G. J. Pilla, Report No. NADC-82032-60, March, 1982.
6. J. A. Filbey, "Factors Affecting the Durability of Titanium/Epoxy Bonds", Ph. D. Dissertation, Virginia Polytechnic Institute and State University, 1987.
7. B. M. Ditchek, K. R. Breen, and J. D. Venables, "Bondability of Ti Adherends", MML TR-80-17C, Final Report 4/1/79-3/31/80.
8. A. C. Kennedy, R. Kohler, and P. Poole, *Int. J. Adhes. and Adhes.* **3,** 133 (1983).
9. J. A. Filbey, J. P. Wightman, and D. J. Progar, *J. Adhesion* **24,** 227 (1987).
10. A. M. Cheng, "Anodic Oxide Formation on Ti-6Al-4V in Chromic Acid for Adhesive Bonding", M.S. Thesis, Virginia Polytechnic Institute and State University, 1983.
11. M. Ditchek, *et al.,* "Bondability of Ti Adherends", *12th National SAMPE Technical Conference,* Oct. 7-9, 1980, pp. 882-895.
12. D. E. Packham, in *Adhesion Aspects of Polymeric Coatings,* K. L. Mittal, Ed. (Plenum Publ. Co. N. Y., 1983).
13. W. Brockmann, O.-D. Hennemann, and H. Kollek, in *Adhesive Joints,* K. L. Mittal, Ed. (Plenum Publ. Co., N.Y., 1984).
14. M. Natan and J. D. Venables, "Bondability of Ti Adherends", MML TR-82-20C, Final Report 8/15/81-8/15/82.
15. R. F. Wegman and D. W. Levi, "Evaluation of Titanium Prebond Treatments by Stress Durability Testing", *27th National SAMPE Symposium,* May 4-6, 1982, pp. 440-452.
16. S. R. Brown, "An Evaluation of Titanium Bonding Pretreatments with a Wedge Test Method", *ibid.,* pp. 363-376.

Appendix A

Chromic Acid Anodization (CAA)

1. Gritblast with an Econoline gritblaster at approximately 100 psi and hold approximately 5 cm from the coupon.
2. Wipe the coupons with methyl ethyl ketone, MEK.
3. Soak in aqueous sodium hydroxide solution (13 g/250 ml) at 70°C for 5 min.
4. Rinse three times in deionized water.
5. Pickling step: Immerse in pickle solution (15 ml conc. HNO_3, 3 ml 49% w/w HF, 82 ml H_2O.
6. Rinse three times in deionized water.

7. Anodize at room temperature for 20 min at 10 V, 26.9 amp/m^2 (2.5 amp/ft^2) in a chromic acid solution (50 g/1000 ml) with Ti–6Al–4V as the cathode. 49% w/w HF is added to attain the desired current density.
8. Rinse three times in deionized water, soaking for 5 min in the final rinse.
9. Blow dry with prepurified nitrogen gas until visibly dry.

Phosphate/Fluoride Etch (P/F)

1. Gritblast as above.
2. Wipe with MEK.
3. Soak in Sprex AN-9 or Super Terj solution (30 g/1000 ml) at 80°C for 15 min.
4. Rinse three times in deionized water.
5. Immerse in pickle solution (31 ml 49% w/w HF, 213 ml conc HNO_3/1000 ml) at room temperature for 2 min.
6. Rinse three times in deionized water.
7. Soak in phosphate fluoride solution (50.5 g Na_3PO_4, 20.5 g KF, 29.1 ml 49% w/w HF/1000 ml) at room temperature for 2 min.
8. Rinse three times in deionized water.
9. Soak in deionized water at 65°C for 15 min.
10. Blow dry as above.

TURCO Basic Etch (TURCO)

1. Gritblast as above.
2. Wipe with MEK.
3. Soak in TURCO 5578 solution (37.6 g/1000 ml) at 70–80°C for 5 min.
4. Rinse three times in deionized water.
5. Soak in TURCO 5578 solution (360 g/1000 ml) at 80–100°C for 10 min.
6. Rinse three times in deionized water.
7. Soak in deionized water at 60°–70°C for 2 min.
8. Blow dry as described above.

Sodium Hydroxide Anodization (SHA)

1. Gritblast as above.
2. Rinse with methanol or acetone.
3. Immerse in Super Terj solution (30 g/1000 ml) at 80°C for 15 min.
4. Rinse three times in deionized water.
5. Soak in water at 50°–60°C for 15 min.
6. Anodize at 20°C for 30 min at 10 V in 5.0 M aqueous sodium hydroxide solution with Ti–6Al–4V as cathode. The current density is not controlled.
7. Rinse in running tap water for 20 min.
8. Blow dry as above.